Research article JHEP|Reports

Therapeutic targeting of adipose tissue macrophages ameliorates liver fibrosis in non-alcoholic fatty liver disease

Authors

Celia Martínez–Sánchez, Octavi Bassegoda, Hongping Deng, Xènia Almodóvar, Ainitze Ibarzabal, Ana de HollandaRaquel–Adela Martínez García de la Torre, Delia Blaya, Silvia Ariño, Natalia Jiménez-Esquivel, Beatriz Aguilar-Bravo, Julia Vallverdú, Carla Montironi, Oscar Osorio-Conles, Yiliam Fundora, Francisco Javier Sánchez Moreno, Alicia G. Gómez-Valadés, Laia Aguilar-Corominas, Anna Soria, Elisa Pose, Adrià Juanola, Marta Cervera, Martina Perez, Virginia Hernández-Gea, Silvia Affò, Kelly S. Swanson, Joana Ferrer-Fàbrega, Jose Maria Balibrea, Pau Sancho-Bru, Josep Vidal, Pere Ginès, Andrew M. Smith, Isabel Graupera, Mar Coll

Correspondence

igraupe@clinic.cat (I. Graupera), mdcoll@clinic.cat (M. Coll).

Graphical abstract

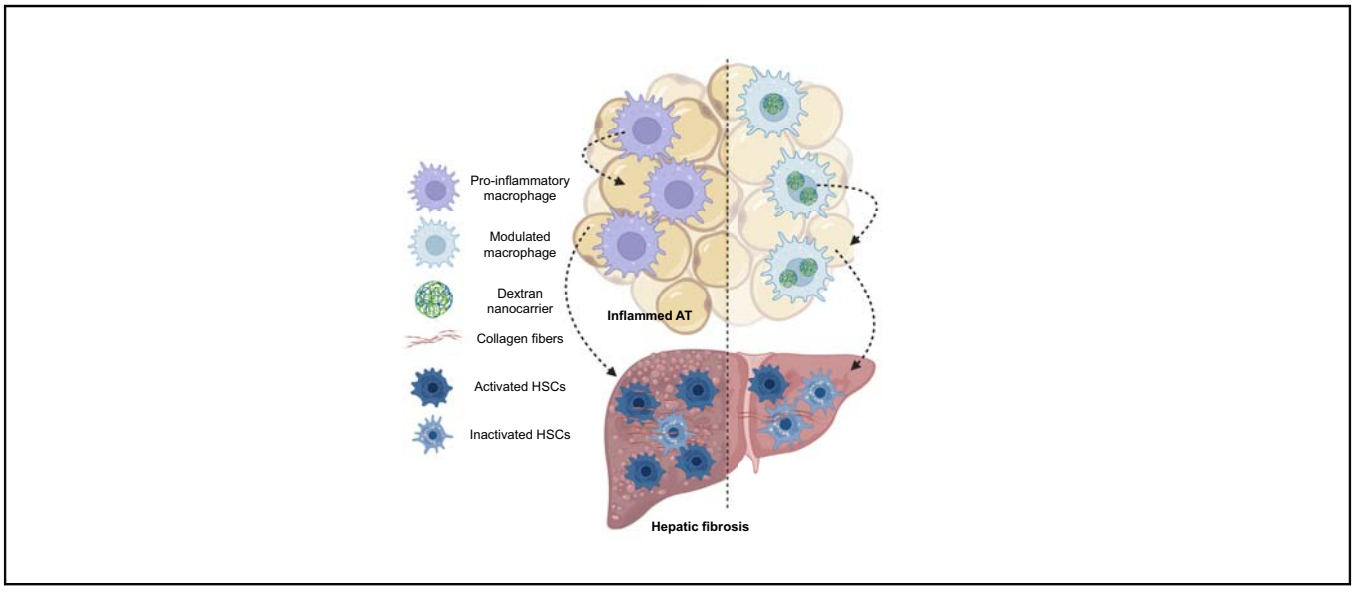

Highlights

- Pro-inflammatory ATMs are associated with fibrosis in patients with NAFLD.
- Dextran coupled with dexamethasone administered i.p. selectively target ATMs.
- Long-term modulation of ATMs reduces their pro-inflammatory phenotype in obese and NASH mice.
- Modulation of ATMs reduces hepatic fibrosis by attenuating hepatic stellate cell activation.

Impact and implications

We report that human adipose tissue pro-inflammatory macrophages correlate with hepatic fibrosis in non-alcoholic fatty liver disease (NAFLD). Furthermore, the modulation of adipose tissue macrophages (ATMs) by dextran-nanocarrier conjugated with dexamethasone shifts the pro-inflammatory phenotype of ATMs to an anti-inflammatory phenotype in an experimental murine model of non-alcoholic steatohepatitis. This shift ameliorates adipose tissue inflammation, hepatic inflammation, and fibrosis. Our results highlight the relevance of adipose tissue in NAFLD pathophysiology and unveil ATMs as a potential target for NAFLD.

https://doi.org/10.1016/j.jhepr.2023.100830

Research article

JHEP Reports

Therapeutic targeting of adipose tissue macrophages ameliorates liver fibrosis in non-alcoholic fatty liver disease

Celia Martínez–Sánchez,[1,2] Octavi Bassegoda,[1,3] Hongping Deng,[4,5,6] Xènia Almodóvar,[1] Ainitze Ibarzabal,[1,7,8,9] Ana de Hollanda,[1,7,9] Raquel–Adela Martínez García de la Torre,[1] Delia Blaya,[1] Silvia Ariño,[1,2] Natalia Jiménez-Esquivel,[3] Beatriz Aguilar-Bravo,[1] Julia Vallverdú,[2] Carla Montironi,[10] Oscar Osorio-Conles,[11] Yiliam Fundora,[12] Francisco Javier Sánchez Moreno,[12] Alicia G. Gómez-Valadés,[13] Laia Aguilar-Corominas,[1] Anna Soria,[1,3] Elisa Pose,[1,2,3] Adrià Juanola,[1,2,3] Marta Cervera,[1] Martina Perez,[1,3] Virginia Hernández-Gea,[1,2,3] Silvia Affò,[1] Kelly S. Swanson,[6,14] Joana Ferrer-Fàbrega,[2,15,16,17,18] Jose Maria Balibrea,[19] Pau Sancho-Bru,[1,2] Josep Vidal,[1,7,11] Pere Ginès,[1,2,3,12] Andrew M. Smith,[4,20,21,22,23] Isabel Graupera,[1,2,3,†,*] Mar Coll[18,†,*]

[1]*Fundació de Recerca Clínic Barcelona-Institut d'Investigacións Biomèdiques August Pi i Sunyer (FCRB-IDIABPS), Barcelona, Spain;* [2]*Centro de Investigación Biomédica en Red de Enfermedades Hepáticas y Digestivas (CIBERehd), Madrid, Spain;* [3]*Liver Unit, Hospital Clínic of Barcelona, Faculty of Medicine, University of Barcelona, Barcelona, Spain;* [4]*Micro and Nanotechnology Laboratory, University of Illinois at Urbana-Champaign, Urbana, Illinois, USA;* [5]*Shanghai Frontiers Science Center for Chinese Medicine Chemical Biology, Institute of Interdisciplinary Integrative Medicine Research, Shanghai University of Traditional Chinese Medicine, Shanghai, China;* [6]*Division of Nutritional Sciences, University of Illinois at Urbana-Champaign, Urbana, Illinois, USA;* [7]*Obesity Unit, Endocrinology and Nutrition Department, Hospital Clínic de Barcelona, Barcelona, Spain;* [8]*Gastrointestinal Surgery Department, Hospital Clínic de Barcelona, Barcelona, Spain;* [9]*Centro de Investigación Biomédica en Red de la Fisiopatología de la Obesidad y Nutrición (CIBEROBN), Instituto de Salud Carlos III (ISCIII), Madrid, Spain;* [10]*Molecular Biology Core & Pathology Department, Hospital Clínic of Barcelona, Spain;* [11]*Centro de Investigación Biomédica en Red de Diabetes y Enfermedades Metabólicas Asociadas (CIBERDEM), Instituto de Salud Carlos III (ISCIII), Madrid, Spain;* [12]*Department of General and Digestive Surgery, Hospital Clinic de Barcelona, Barcelona, Spain;* [13]*Neuronal Control of Metabolism (NeuCoMe) Laboratory, Fundació de Recerca Clínic Barcelona-Institut d'Investigacions Biomèdiques August Pi i Sunyer (FCRB-IDIABPS), Barcelona, Spain;* [14]*Department of Animal Sciences, University of Illinois at Urbana-Champaign, Urbana, Illinois, USA;* [15]*Barcelona Clínic Liver Cancer Group (BCLC), IDIBAPS, Barcelona, Spain;* [16]*Hepatic Oncology Unit, Hospital Clínic, Barcelona, Spain;* [17]*Hepatobiliopancreatic Surgery and Liver and Pancreatic Transplantation Unit, Department of Surgery, Institute Clínic of Digestive and Metabolic Diseases (ICMDiM), Hospital Clínic, Barcelona, Spain;* [18]*Department of Medicine, University of Barcelona, Barcelona, Spain;* [19]*Endocrine, Metabolic & Bariatric Surgery Unit, Germans Trias i Pujol Hospital, Autonomous University of Barcelona, Barcelona, Spain;* [20]*Department of Bioengineering, University of Illinois at Urbana-Champaign, Urbana, IL, USA;* [21]*Cancer Center at Illinois, University of Illinois at Urbana-Champaign, Urbana, IL, USA;* [22]*Carle Illinois College of Medicine, Urbana, IL, USA;* [23]*Department of Materials Science and Engineering, University of Illinois at Urbana-Champaign, Urbana, IL, USA*

JHEP Reports **2023.** https://doi.org/10.1016/j.jhepr.2023.100830

Background & Aims: : The accumulation of adipose tissue macrophages (ATMs) in obesity has been associated with hepatic injury. However, the contribution of ATMs to hepatic fibrosis in non-alcoholic fatty liver disease (NAFLD) remains to be elucidated. Herein, we investigate the relationship between ATMs and liver fibrosis in patients with patients with NAFLD and evaluate the impact of modulation of ATMs over hepatic fibrosis in an experimental non-alcoholic steatohepatitis (NASH) model.

Methods: Adipose tissue and liver biopsies from 42 patients with NAFLD with different fibrosis stages were collected. ATMs were characterised by immunohistochemistry and flow cytometry and the correlation between ATMs and liver fibrosis stages was assessed. Selective modulation of the ATM phenotype was achieved by *i.p.* administration of dextran coupled with dexamethasone in diet-induced obesity and NASH murine models. Chronic administration effects were evaluated by histology and gene expression analysis in adipose tissue and liver samples. *In vitro* crosstalk between human ATMs and hepatic stellate cells (HSCs) and liver spheroids was performed.

Results: Patients with NAFLD presented an increased accumulation of pro-inflammatory ATMs that correlated with hepatic fibrosis. Long-term modulation of ATMs significantly reduced pro-inflammatory phenotype and ameliorated adipose tissue inflammation. Moreover, ATMs modulation was associated with an improvement in steatosis and hepatic inflammation and significantly reduced fibrosis progression in an experimental NASH model. *In vitro*, the reduction of the pro-inflammatory

Keywords: Dextran dexamethasone conjugates; Non-alcoholic steatohepatitis; Liver injury; Adipose tissue inflammation; Nanoparticle; Nanomedicine; Targeted therapy; Drug delivery.

Received 11 October 2022; received in revised form 2 May 2023; accepted 5 June 2023; available online 27 June 2023

† These authors are co-senior authors and equally contributed to this work.

* Corresponding authors. Addresses: Liver Unit, Hospital Clínic Barcelona, Villarroel, 170, 08036 Barcelona, Spain. Tel.: +34 932272846 (I. Graupera); Medicine Department, Faculty of Medicine, University of Barcelona, Centre Esther Koplowitz, C/Rosselló, 149-153, third floor, 08036 Barcelona, Spain. Tel.: +34 932274535 Ext. 4535 (M. Coll).

E-mail addresses: igraupe@clinic.cat (I. Graupera), mdcoll@clinic.cat (M. Coll).

phenotype of human ATMs with dextran–dexamethasone treatment reduced the secretion of inflammatory chemokines and directly attenuated the pro-fibrogenic response in HSCs and liver spheroids.
Conclusions: Pro-inflammatory ATMs increase in parallel with fibrosis degree in patients with NAFLD and their modulation in an experimental NASH model improves liver fibrosis, uncovering the potential of ATMs as a therapeutic target to mitigate liver fibrosis in NAFLD.
Impact and implications: We report that human adipose tissue pro-inflammatory macrophages correlate with hepatic fibrosis in non-alcoholic fatty liver disease (NAFLD). Furthermore, the modulation of adipose tissue macrophages (ATMs) by dextran-nanocarrier conjugated with dexamethasone shifts the pro-inflammatory phenotype of ATMs to an anti-inflammatory phenotype in an experimental murine model of non-alcoholic steatohepatitis. This shift ameliorates adipose tissue inflammation, hepatic inflammation, and fibrosis. Our results highlight the relevance of adipose tissue in NAFLD pathophysiology and unveil ATMs as a potential target for NAFLD.

Introduction

Non-alcoholic fatty liver disease (NAFLD) is the most prevalent chronic liver disease worldwide and is characterised by fatty acid accumulation within hepatocytes that eventually can lead to lipotoxicity, inflammation, and fibrogenesis promoting scar deposition.[1,2] Several studies have shown that the fibrosis stage is the most important determinant of liver-related progression and mortality for patients with NAFLD.[3–5] Therefore, halting fibrosis progression or reversing fibrosis may prevent liver-related outcomes of NAFLD such as the risk of developing cirrhosis or decompensation.

Together with intrahepatic signals, extrahepatic mediators from other organs such as the gut microbiome and adipose tissue, may play a critical role in the development of NAFLD.[6] Indeed, in the context of obesity, adipose tissue (AT) is characterised by adipocyte hypertrophy together with marked infiltration of macrophages (ATMs) with a pro-inflammatory phenotype, defined as $CD11c^+$ macrophages, which are found in crown-like structures surrounding dead adipocytes.[7–10] Moreover, adipose tissue inflammation and the infiltration of pro-inflammatory ATMs impair systemic insulin activity and correlate with worse outcomes in cardiovascular diseases.[11,12] The potential role of ATMs in NAFLD was first reported by Bijnen *et al.* when they transplanted visceral adipose tissue (VAT) from obese to lean mice and observed an accumulation of hepatic neutrophil and macrophage cells contributing to the development of steatohepatitis.[13] In humans, very little is known about the pathogenic relationship between ATMs content and NAFLD progression.[14] It has been reported that both the gene expression of pro-inflammatory markers in the adipose tissue and the number of ATMs are associated with the progression from non-alcoholic fatty liver to non-alcoholic steatohepatitis (NASH).[10,15–17] Nevertheless, although the role of pro-inflammatory ATMs in systemic and liver inflammation in obese patients has been described,[18,19] whether $CD11c^+$ ATMs directly contribute to hepatic injury and fibrosis in the context of NAFLD remains unclear.

Herein, by characterising paired adipose tissue and liver samples of patients with NAFLD we assessed the accumulation of pro-inflammatory ATMs and evaluated their association with liver fibrosis stages. Furthermore, we investigated the direct effect of reducing the pro-inflammatory phenotype of ATMs on liver fibrosis in mouse models of NAFLD and human hepatic stellate cells (HSCs). Overall, our study reveals a direct association between increased accumulation of macrophages in the adipose tissue and the degree of liver fibrosis in patients with NAFLD and shows that the modulation of ATMs can halt the liver fibrogenesis machinery highlighting the potential of ATMs as a therapeutic target to mitigate liver damage in this disease.

Patients and methods

Patient cohort

We included a cohort of 42 patients with NAFLD at different disease stages: patients with steatosis and no fibrosis (n = 24); patients with mild fibrosis, stage F1–F2 (n = 6); and patients with advanced fibrosis, stage F3–F4 (n = 12). NAFLD was diagnosed according to current guidelines,[20] and the liver fibrosis stage was classified according to the NASH Clinical Research Network (CRN) Scoring system.[21] Patient characteristics are detailed in Table 1. VAT and liver tissue were collected at the time of bariatric surgery, liver segmentectomy, or liver transplant at the Hospital Clinic of Barcelona. Adipose tissue was excised for RNA analysis, embedded in paraffin (Sigma, St. Louis, MO, USA, #1.11609.9025), or digested for the isolation of fresh ATMs. The study protocol followed the ethical guidelines of the 1975 Declaration of Helsinki and was approved by the Hospital Clinic Research Ethics Committee (HCB/2019/0458). All patients provided written informed consent to participate in the study.

Isolation and culture of human ATMs

Adipose tissue biopsies were processed as previously described.[22] Briefly, after digesting the sample using collagenase type 2 (Worthington, Lakewood, NJ, USA, #LS004176), erythrocytes were lysed (BD Bioscience, San Jose, CA, USA, #555899) and the human ATM fraction was enriched from the stromal vascular fraction after being allowed to attach for 1 h (4.54×10^5 cells/cm^2). Isolated ATMs were kept in culture under basal conditions or polarised towards a pro-inflammatory state and after 24 h the secretome was collected for further experiments. The pro-inflammatory state was mimicked *in vitro* by adding lipopolysaccharides (LPS) (100 ng/ml; Sigma, #L2637) and interferon gamma (IFN_γ) (20 ng/ml; BD Biosciences, #554617) to the medium overnight. Next, cells were treated with free dextran (FD) or dextran–dexamethasone (DD) (0.05 mg/ml) as previously described,[23] for an additional 6 h with or without continued stimulation with pro-inflammatory cytokines according to the experimental group. Conditioned medium from treated ATM and RNA were collected and stored for further analysis.

Table 1. Baseline characteristics of the NAFLD cohort.

	Fibrosis stage			
	F0 (n = 24)	F1–F2 (n = 6)	F3–F4 (n = 12)	*p* value
Demographics				
Age, median (IQR)	53 (44–63)	58 (50–65)	59 (55–62)	0.012
Sex, male, n (%)	40.9%	50%	75%	n.s.
BMI (kg/m^2), median (IQR)	42 (40–49)	41 (38–44)	32 (27–39)	0.012
Weight (kg), median (IQR)	125 (110–133)	110 (99–117)	92 (77–105)	0.028
Waist circumference (cm), median (IQR)	130 (123–132)	121 (117–124)	108 (96–127)	n.s.
Fibrosis severity, median (IQR)				
NFS	−1.1 (−1.8 to −0.3)	n1.5 (-1.9 to -1.1)	1.55 (0 to -2.4)	0.0007
FIB–4	0.7 (0.6 −1.1)	1.0 (0.8–1.4)	5.25 (2.5–11.2)	<0.0001
Fibroscan value (kPa)*	9.5 (7.2–11.7)	7.0 (6.5–8.8)	25.20 (11.7–27.4)	0.015
CAP value (db/m^2)*	338.5 (334.2–342.7)	350 (328–388)	269 (248–352)	n.s.
Laboratory parameters, median (IQR)				
ALP (U/L)	81 (74–93)	72 (70 –85)	95 (90–120)	n.s.
AST (U/L)	21 (18–26)	27 (24–30)	48 (42–58)	<0.0001
ALT (U/L)	26 (22–33)	35 (34–39)	35 (25–53)	0.044
Arterial hypertension (%)	37.5%	83.3%	91.67%	n.s.
Diabetes (%)	18.2%	16.7%	9.1%	n.s.
Albumin (g/dl)	4.5 (4.5–4.6)	4.5 (4.5–4.7)	3.5 (2.8–4.1)	0.001
GGT (U/L)	32 (22–47)	50.5 (34–67.7)	34 (30.0–79.5)	n.s.
Platelets (× 10^9/L)	246 (207–299)	284 (254–307)	91 (58–192)	0.000
Glucose (mg/dl)	97 (84–109)	96 (92–106)	100 (88–116)	n.s.
Glycohaemoglobin (%)	5.7 (5.4–6.1)	5.6 (5.5–5.8)	4.7 (4.2–6.4)	n.s.
Triglycerides (mg/dl)	119 (114–156)	148 (130–181)	88.5 (74–123)	0.016
Cholesterol LDL (mg/dl)	123 (98–136)	135 (120–137.2)	99.5 (80–122)	n.s.
Cholesterol HDL (mg/dl)	44 (40–54)	47 (42–49)	44 (35–52)	n.s.

Results are expressed as median and interquartile range (25%–75%). The Kruskal–Wallis test was used to compare groups; *p* values <0.05 were considered significant. We categorised and defined the study participants into those with no fibrosis, F0 (n = 22); mild fibrosis, F1–F2 (n = 6); and advanced fibrosis, F3–F4 (n = 11) as assessed by Isabel Graupera.
ALP, alkaline phosphatase; ALT, alanine aminotransferase; AST, aspartate aminotransferase; CAP, controlled attenuation parameter; FIB-4, fibrosis-4; GGT, gamma-glutamyl transferase; HTN, hypertension; NAFLD, non-alcoholic fatty liver disease; NFS, NAFLD fibrosis score.
* Given clinical limitations significant values were determined using the Mann–Whitney test to compare F1–F2 and F3–F4 values.

Flow cytometry analysis

Human ATMs used for flow cytometry analysis were detached using Tryple solution (ThermoFisher, Waltham, MA, USA, #12604021) and incubated with a mixed panel of antibodies (CTAT methods) for 20 min at 4 °C in the dark. Next, samples were analysed with the FACSCanto™ II system (BD Biosciences) and FlowJo v10.2 (BD Biosciences, FlowJo LLC).

Mice models

C57BL/6J mice were purchased from the Jackson Laboratories at 7 weeks of age. The mice were housed in temperature- and humidity-controlled rooms, and maintained on a 12-h/12-h light/dark cycle. At 8 weeks of age, mice were randomly allocated to experimental groups and placed on a high-fat diet (HFD, 60% kcal from fat, Brogaarden, #D12492i) or a high-fat high-cholesterol diet (HFHCD, 60% kcal from fat and supplemented with 0.5% of cholesterol, Brogaarden, #D12011002) for 6 months *ad libitum*. To assess dextran conjugate biodistribution, dextran-FITC (ThermoFisher, #D7136) was administered i.p. twice per week for the last 5 weeks of feeding at a dose of 0.7 mg/kg and 48 h after the last injection the animals were euthanised. Dextran conjugates were synthesised as described in the Supplemental information.[27] The effect of the dextran conjugates was evaluated by distributing animals into (1) mice receiving HFD and treated with free dextran (Obese FD) (n = 10); (2) mice receiving HFD and treated with dextran–dexamethasone (Obese DD) (n = 7); (3) mice receiving HFHCD and treated with free dextran (NASH FD) (n = 10); and (4) mice receiving HFHCD and treated with dextran–dexamethasone (NASH DD) (n = 10). Liver and adipose tissue sample processing details are described in Supplemental methods.[38] All experimental procedures were approved by the Ethics Committee of Animal Experimentation of the University of Barcelona and were performed according to the National Institute of Health's Guide for the Care and Use of Laboratory Animals.

Hepatic stellate cells and liver spheroids *in vitro* experiments

Human induced pluripotent stem cells (iPSCs) were differentiated to HSCs (iPSC-HSC) following the protocol described by Vallverdú *et al.*[24] iPSC-HSC were seeded (60,000 cells/well) and cultured until a confluence of 60–70% was reached. Then, iPSC-HSCs were incubated with 200 μl of conditioned medium from human ATMs from patients with NAFLD with and without fibrosis or with the secretome of ATMs from obese patients treated with FD or DD (0.05 mg/ml) and collected for gene expression analysis after 48 h.

Liver spheroids were generated in ultra-low attachment plates using $HepG_2$ cells and iPSC-HSCs in a 2:1 ratio as previously described.[24] Liver spheroids were then stimulated with 200 μl of conditioned medium from human ATMs treated with FD or DD for 72 h.

Statistical analysis

Statistical analysis was performed using GraphPad Prism 5.0 (San Diego, CA, USA). Values were expressed as means ± SD. Statistical differences between groups were analysed using the non-parametric Mann-Whitney test or ANOVA when required. Paired samples were analysed using the Wilcoxon test. A *p* value ≤0.05 was considered statistically significant. Correlations

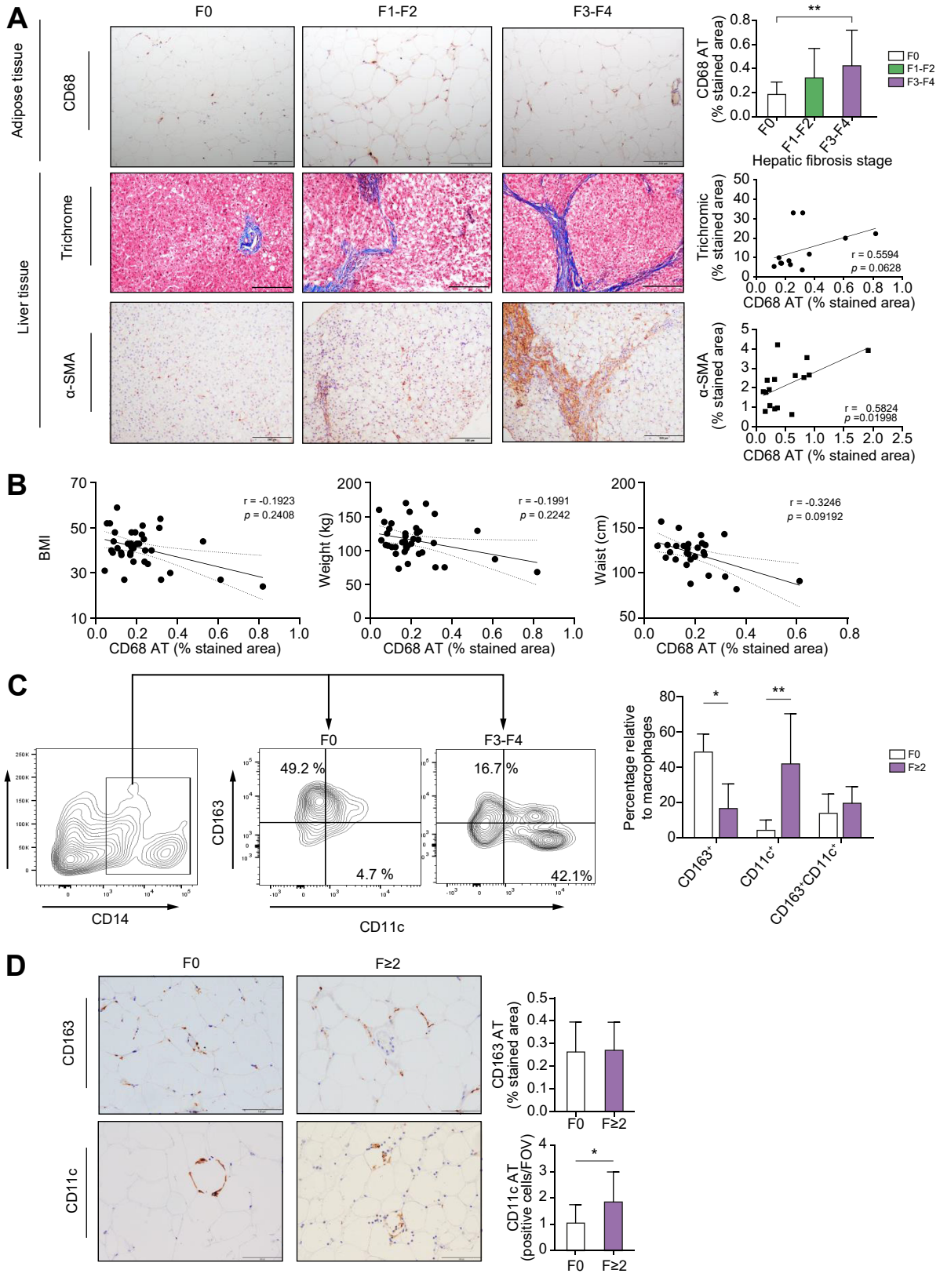

Fig. 1. Pro-inflammatory ATMs increase with hepatic fibrosis in patients with NAFLD. (A) Immunohistochemical analysis of ATMs in the adipose tissue and hepatic fibrosis assessment by trichrome or α-SMA staining in liver biopsies. Scale bar: 200 μm. (B) Correlation of percentage of ATMs with the BMI, body weight, and waist circumference of patients with NAFLD: F0 (n = 20); F1–F2 (n = 6) and F3–F4 (n = 12). (C) Quantification of the percentage of pro-inflammatory ($CD14^+CD11c^+$); anti-inflammatory ($CD14^+CD163^+$) and intermediate ($CD14^+CD11c^+CD163^+$) ATMs in patients with NAFLD with different fibrosis stages: F0

between variables were evaluated using Spearman's rank correlations.

Results

Human pro-inflammatory ATM are directly associated with fibrosis stage in NAFLD

We assessed by immunohistochemistry the accumulation of macrophages in adipose tissue in patients with NAFLD with different hepatic fibrosis stages. Table 1 shows the characteristics of the cohort of patients with NAFLD stratified according to liver fibrosis ranging from F0 to F4. As shown in Fig. 1A we observed that the area occupied by ATMs ($CD68^+$ stained cells) increased progressively along with the liver fibrosis stage. In fact, patients without liver fibrosis displayed half the number of macrophages than those with advanced fibrosis stages F3–F4 (0.18% ± 0.025 *vs.* 0.32% ± 0.08, $p = 0.0037$). Accordingly, we identified a positive correlation between the abundance of macrophages accumulated in the AT and the area of collagen and α-smooth muscle actin (α-SMA) in liver sections. Interestingly, we found a negative correlation tendency between ATM number and the BMI, weight, and waist circumference, suggesting that adipose tissue macrophage infiltration was associated with fibrosis independently of the obesity grade (Fig. 1B). To further investigate whether there was a specific ATM phenotype associated with liver fibrosis, we used flow cytometry to evaluate the abundance of anti-inflammatory ($CD14^+CD163^+$), intermediate ($CD14^+CD11c^+CD163^+$) and pro-inflammatory ($CD14^+CD11c^+$) subsets of ATMs in patients with NAFLD with and without liver fibrosis. Interestingly, patients with advanced liver fibrosis exhibited a significant reduction of the anti-inflammatory ATM subtype (49.23% ± 3.95 *vs.* 16.73% ± 6.16, $p = 0.0043$) together with a significant increase of the pro-inflammatory ATMs subtypes (4.70% ± 1.87 *vs.* 42.10% ± 11.56, $p = 0.008$) compared with patients without fibrosis. We did not observe any differences in ATM subtype having an intermediate phenotype between groups (Fig. 1C). Moreover, the immunochemistry staining of CD163 and CD11c markers in the AT from patients with NAFLD confirmed these results (Fig. 1D). As AT fibrosis may be linked to NAFLD, we assessed the gene expression of *PDGFC, ACTA2, COL3A1, COL4A1, COL6A3,* and *MMP9* in the AT and there were no differences among patients with different liver fibrosis stages. Furthermore, we performed Sirius Red staining on AT histology sections and did not find any differences between patients with NAFLD with and without fibrosis (Fig. S1). Together, these findings suggest that the abundance of pro-inflammatory ATM is associated with liver fibrosis progression in patients with NAFLD.

Dextran nanocarrier is predominantly captured by macrophages of the inflamed adipose tissue of NASH and obese mice

First, we confirmed that after a 6-month diet of HFD or HFHCD, both animal models reproduced the key clinical and histological features of obesity and NASH, respectively. Both models presented a significant increase in body and adipose tissue weight without showing differences between groups (Fig. S2A). No differences in terms of serum liver enzyme levels (Aspartate aminotransferase [AST], alanine aminotransferase [ALT], or lactate dehydrogenase [LDH]) were found between experimental groups (Fig. S2B). Blinded histopathological analysis of the liver showed that the NASH model (HFHCD) presented a higher steatosis grade, lobular inflammation, and fibrosis deposition compared with the obese model (Fig. S2C and D).

Next, we used a strategy based on acute i.p. administration of nanoscale polysaccharide nanocarriers that selectively target macrophages in VAT.[23,25] The uptake of the nano-transporter by ATMs and liver macrophages (HepMs) was evaluated by flow cytometry and immunofluorescence 48 h after injection. Fluorescent signals co-localised with the macrophage marker F4/80 in both tissues and in freshly isolated macrophages, indicating that the nanocarrier was engulfed by ATMs and their counterparts in the liver (Fig. 2A). Notably, flow cytometry analysis showed that the nanocarrier was predominantly captured by ATMs compared with liver macrophages in NASH (23.16% ± 2.40 *vs.* 7.37% ± 0.45; $p = 0.0001$) and obesity (13.30% ± 1.20 *vs.* 5.18% ± 1.05, $p = 0.0098$) models. Interestingly, the capacity of ATMs to phagocytise the nanocarrier was twofold higher in NASH mice compared with obese mice, confirming that the dextran nanocarrier principally targets inflamed tissues (Fig. 2B and Fig. S3). We next evaluated whether there was a specific ATM subtype responsible for dextran phagocytosis. By immunofluorescence analysis we assessed the co-staining of dextran with the anti-inflammatory marker (CD163), the pro-inflammatory marker (CD11c), and the lipid-associated macrophage marker (CD9) of ATMs. As shown in Fig. 2C, there was a clear engulfment in the pro-inflammatory phenotype, whereas no or slight uptake was detected in other phenotypes. Overall, these results demonstrate that the dextran nanocarrier administered through the peritoneal cavity predominantly targets the macrophage population in the adipose tissue and is mainly captured by pro-inflammatory macrophages.

Long-term dextran-dexamethasone treatment ameliorates adipose tissue inflammation by modulating ATM phenotype

Dexamethasone conjugated with DD or FD was administered twice per week for 5 weeks to obese and NASH mice (Fig. 3A). After starting DD administration, obese and NASH animals began to progressively lose weight. At the end of the treatment, the reduction in the body weight of the animals with the anti-inflammatory treatment (DD) was higher than those groups receiving FD, which was accompanied by a significant reduction in the fat deposits (Fig. 3B and Fig. S4). To examine the effects of chronic DD treatment on AT morphology and function we evaluated the influence of FD and DD on adipocyte size and number and found no differences between control and treated animals (Fig. 3C). Subsequently, we assessed by gene expression of the main lipolytic and lipogenic genes and found that there were no differences between treated (DD) and control groups (FD) (Fig. 3D). Finally, we focused on evaluating the changes promoted by our DD treatment on the inflammatory milieu in the adipose tissue. All key inflammatory markers assessed (*Il10, Il1b, Ccl2, F4/80, Ifng, Il6; Tnfa,* and *Nos2*) presented significantly

(n = 7) and F3–F4 (n = 7). (D) Immunohistochemical analysis of CD163 and CD11c staining in adipose tissue F0 (n = 15) and F≥2 (n = 16). Data represented as mean ± SD. Scale bar: 100 μm. Correlations were performed with Spearman's correlation. The Mann–Whitney test was used to compare patients at different stages. $^*p$ <0.05, $^{**}p$ <0.01 by ANOVA (A), Mann–Whitney test (C, D). α-SMA, α-smooth muscle actin; AT, adipose tissue; ATM, adipose tissue macrophages; FOV, field of view; NAFLD, non-alcoholic fatty liver disease.

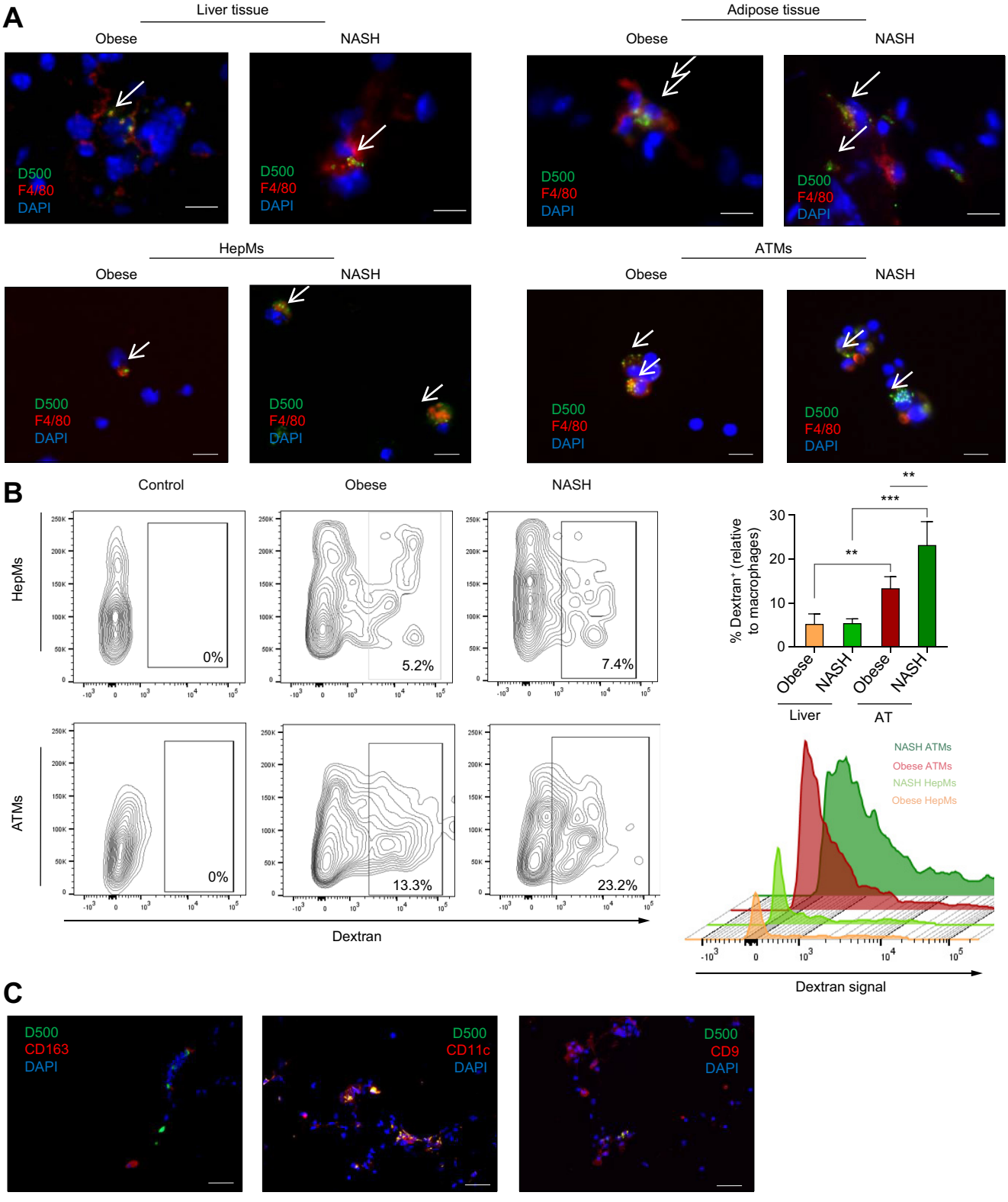

Fig. 2. Dextran nanocarriers are captured by macrophages and predominantly retained in the adipose tissue of the NASH animals. (A) Representative immunofluorescence of dextran 500 (green) phagocytised by macrophages (F4/80, red) in the liver and adipose tissue and in isolated macrophages in obese and NASH models. Scale bar: 20 μm. (B) Flow cytometry analysis of the dextran ($F4/80^+CD11b^+dextran^+$) captured by isolated macrophages from liver and adipose tissue of obese and NASH model animals (n = 5, each group). Histogram of mean intensity fluorescence of the dextran signal captured by macrophages is also shown. Data represented as mean ± SD. (C) Representative immunofluorescence of dextran 500 (green) and anti-inflammatory ATMs (CD163, red); pro-inflammatory ATMs (CD11c, red) or lipid associated macrophages (CD9, red) in adipose tissue in NASH mice. Scale bar: 100 μm. ANOVA test. $^{**}p$ <0.01. AT, adipose tissue; ATMs, adipose tissue macrophages; D500, Dextran 500 kDa; HepMs, hepatic macrophages; NASH, non-alcoholic steatohepatitis.

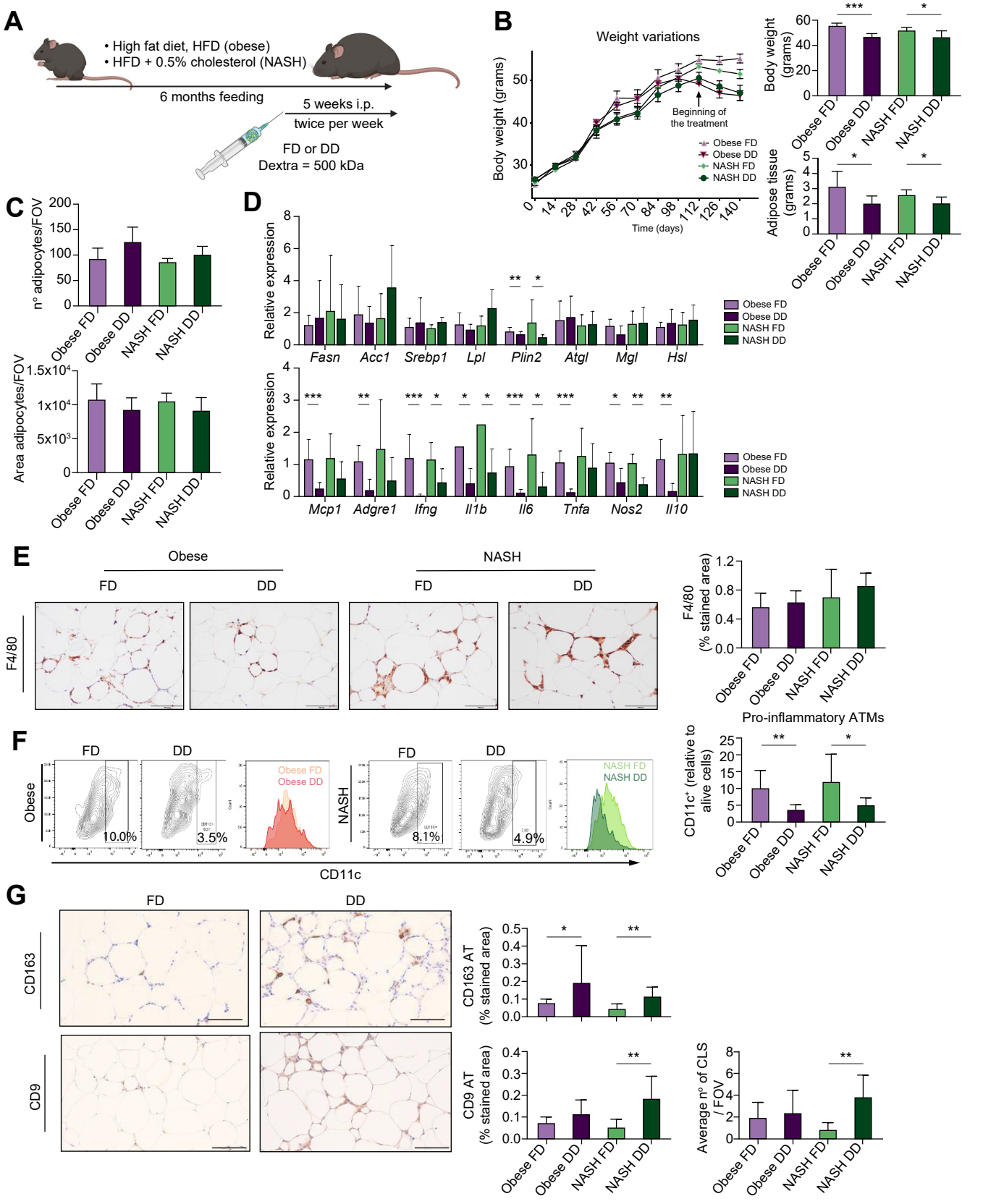

Fig. 3. Chronic dextran-dexamethasone treatment modulates pro-inflammatory ATMs and adipose tissue inflammation in obese and NASH models. (A) Experimental design of the model protocol. (B) Body weight measurements during the experimental protocol in the obese and NASH models. The arrow indicates the beginning of the treatment. Body weight and peritoneal fat pads were weighed at the time of the euthanisation of all experimental groups. (C) Relative number of adipocytes and the average area of adipocytes per field of view (FOV). (D) Relative gene expression of key lipid metabolic and inflammatory markers in

reduced expression in the obese model after DD treatment compared with the FD group. The changes in the NASH model were more discrete but there was also a significant decrease in the expression of *Infg, Il1b*, *Il6*, *Tnfa,* and *Nos2* when treated with DD compared with FD (Fig. 3D). Interestingly, the reduction observed in the inflammation of AT was not accompanied by a decrease in the number of ATMs as illustrated by the immunohistochemistry quantification of the macrophage population (Fig. 3E). To evaluate whether the reduction of the inflammation was mediated by a modulation of the ATMs phenotype, we assessed the percentage of pro-inflammatory macrophages by flow cytometry analysis of the CD11c marker. A reduction in the $CD11c^+$ population was observed in the adipose tissue in both models treated with DD compared with FD (9.98 ± 1.55 *vs.* 3.54 ± 0.61, $p = 0.002$ and 11.8± 2.52 *vs.* 4.90 ± 0.81, $p = 0.037$) (Fig. 3F). Likewise, expression of the pro-inflammatory mediators *Il6* and *Il1b* significantly decreased in ATMs isolated from animals treated with DD compared with those receiving FD (Fig. S4C). To gain further insight on the effects of our treatment in other ATMs subpopulations we performed immunohistochemical staining using CD9 and CD163 markers. As shown in Fig. 3G there was a significant enrichment of CD9 ATMs and CD163 ATMs in the treated groups (DD) compared with the control groups (FD). Accordingly, we found an increase in crown-like structures in the NASH DD group (p = 0.008) compared with their control group. Taken together these data indicate that *i.p.* administration of DD conjugates reduces the pro-inflammatory phenotype of ATMs, promotes the expression of lipid-associated macrophages and tissue-resident macrophages, and leads to a reduction in the inflammation of AT.

ATMs phenotype modulation improves hepatic histological features of NAFLD

Blinded histopathological analysis of liver sections from obese and NASH models after DD treatment was performed. Interestingly, as shown in Fig. 4A, DD treatment led to a reduction of the steatosis grade from 1–3 towards 0–2 in the NASH model and from 0–2 towards 0–1 in the obese model. Furthermore, we observed a statistically significant reduction of hepatocyte ballooning in the NASH group treated with DD, as well as an improvement in the lobular inflammation in both the obese and NASH animals treated with DD compared with FD. Altogether, NASH animals treated with DD presented a significant reduction in the NAFLD activity score.[26] The improvement of hepatic histological injury upon DD treatment in obese and NASH models was not accompanied by any changes in the circulating levels of liver enzymes (Fig. S4). We further evaluated liver inflammation by assessing the expression of pro-inflammatory cytokines in liver tissue (*Ccl2, Il1b, Tnfa, Ifng,* and *Il6)* and found out that most of the cytokines evaluated were significantly reduced in one or both experimental models after DD treatment (Fig. 4B). Because sustained expression of inducible nitric oxide synthase (iNOS) is a hallmark of chronic liver inflammation, we assessed its expression in liver sections. In agreement with our previous findings, iNOS expression markedly decreased in animals treated with DD compared with those receiving FD in both models. Next, to evaluate whether the treatment influenced immune cell populations, we analysed the abundance of neutrophils, macrophages, and lymphocytes in all experimental groups. Although the percentage of hepatic neutrophils and macrophages did not change in obese and NASH animals, the treatment markedly reduced the number of lymphocytes in both models, as assessed by CD3 staining (Fig. 4C). In addition, we did not observe any significant changes in the pro-inflammatory phenotype of liver macrophages as shown by the percentage of $F4/80^+CD11b^+CD11c^+$ cells assessed by flow cytometry (Fig. 4D). The gene expression analysis of pro-inflammatory mediators *Il6, Il1b, Tnfa,* and *Ifng* on freshly isolated hepatic macrophages showed a consistent trend toward reducing their expression in the NASH model after DD treatment although no significant results were found (Fig. 4E). Taken together, these results demonstrated that chronic DD treatment ameliorated NAFLD-associated liver inflammation without significantly affecting the liver macrophage population.

Dextran-dexamethasone treatment alleviates liver fibrosis

Sirius Red staining of liver sections was used to perform a detailed semi-quantitative analysis of pericellular fibrosis. Interestingly, DD treatment reduced fibrosis in the NASH animals compared with the FD group. This finding was also verified by quantifying the collagen-stained area in liver sections of mice treated with FD or DD (2.35% *vs*. 0.899%, $p = 0.004$) (Fig. 5A). Consistently, we quantified the α-SMA staining and found that DD treatment significantly reduced liver fibrosis in both obese and NASH models (2.14% *vs.* 0.26%, $p = 0.01$ and 2.30% *vs*. 0.74%, $p = 0.0095$ in obese and NASH models, respectively) (Fig. 5B). Gene expression of key markers of HSC activation such as *Col1a1*, *Col1a2*, *Icam1*, *Mmp2,* and *Pdgf* were reduced with chronic DD administration (Fig. 5C), although only *Col1a1* showed a statistically significant reduction in the NASH model. These results highlight the role of extrahepatic inflammatory signals on liver fibrosis and the potential of the modulation of ATMs to reduce fibrosis in NAFLD.

Human ATMs switch their phenotype upon dexamethasone nanocarrier engulfment

We sought to determine whether the reduction of the pro-inflammatory phenotype of ATMs upon DD treatment could be translated into humans. We isolated ATMs from patients who were obese undergoing bariatric surgery and studied their phenotype shift after FD or DD treatment. First, by flow cytometry, we determined the efficiency of human-isolated cells to phagocyte the dextran nanocarrier (72.1%) (Fig. S5). Then, we assessed the phenotypic changes produced in pro-inflammatory and anti-inflammatory ATMs subpopulations after a 24-h treatment with FD or DD. Interestingly, similar to what we observed in our murine models, proinflammatory (CD11c+) macrophages were significantly reduced ($p = 0.0186$) after DD treatment

the adipose tissue of obese and NASH models treated with FD or DD. Expression values are represented as fold change related to FD group (E) Representative immunohistochemical staining of F4/80 in the adipose tissue of treated NASH and obese animals (FD or DD) and its quantification. (F) Representative flow cytometry plots and histograms showing the pro-inflammatory ATMs subset ($F4/80^+CD11b^+CD11c^+$) of the obese and NASH animals after treatment (FD or DD) and their quantification. (G) Representative immunohistochemical staining of CD9 in the AT of NASH animals (FD or DD). Quantification of %CD9 positive area in all experimental animal groups: obese FD (n = 10), obese DD (n = 7); NASH FD (n = 10), and NASH DD (n = 9). Data represented as mean ± SD. Scale bar: 100 μm $^*p$ <0.05; $^{**}p$ <0.01; $^{***}p$ <0.001 by the Mann–Whitney test. DD, dextran-dexamethasone; FD, free dextran; FOV, field of view; NASH, non-alcoholic steatohepatitis.

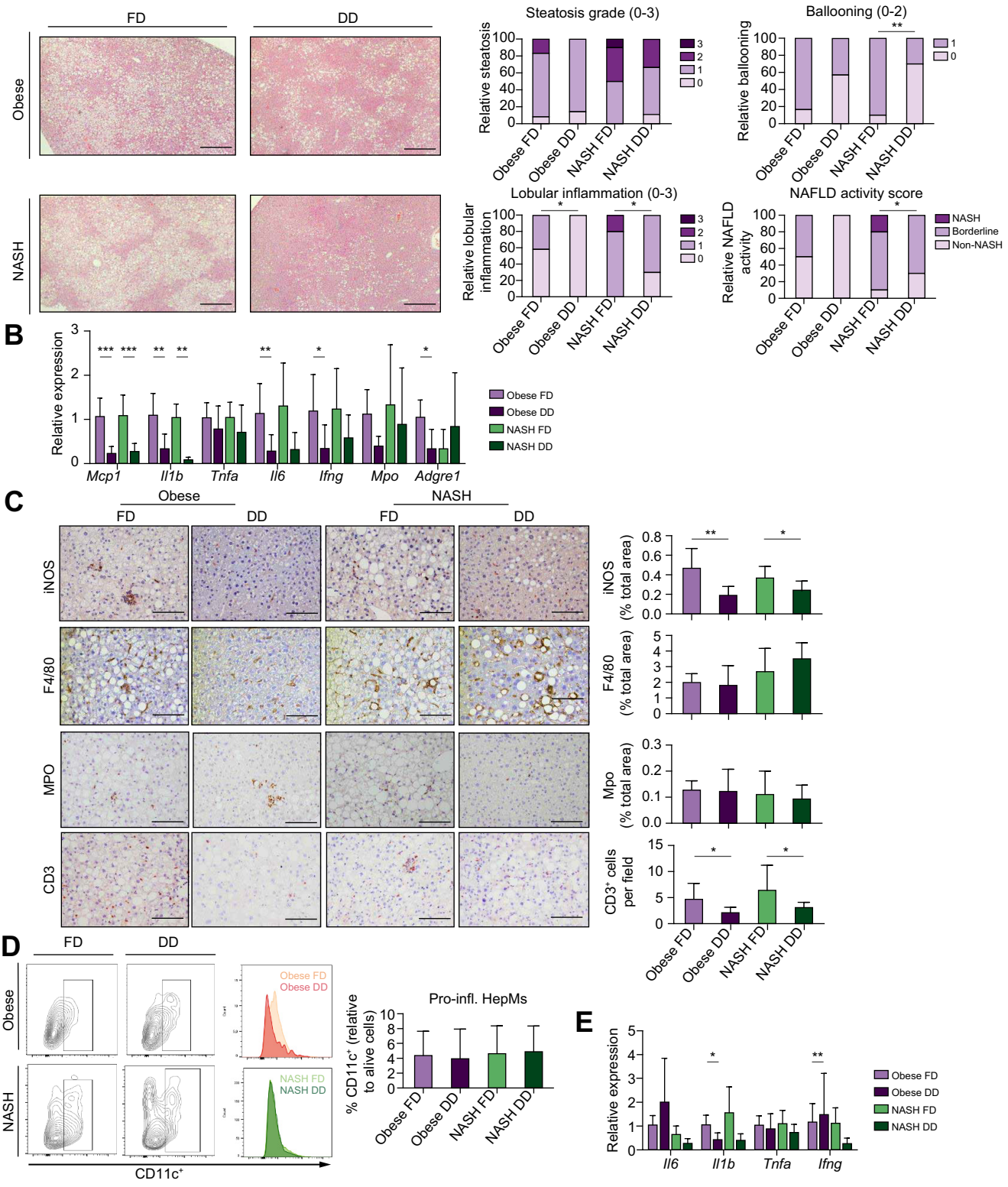

Fig. 4. Long-term dextran-dexamethasone administration reduces hepatic inflammation without affecting the phenotype of liver macrophages. (A) Representative haematoxylin and eosin staining of liver sections of obese or NASH mice after DD treatment. Scale bar: 200 μm. Semi quantitative histological analysis of the steatosis grade, ballooning degree, lobular inflammation grade, and NAFLD activity score in each experimental group. (B) Gene expression levels measured by quantitative PCR of inflammatory markers in liver tissue. (C) Representative immunohistochemical staining of iNOS and immune cell populations such as macrophages (F4/80), neutrophils (MPO), and lymphocytes (CD3) are shown. Scale bar: 50 μm. (D) Determination of liver pro-inflammatory macrophages by flow cytometry determined by the $F4/80^{+}CD11b^{+}CD11c^{+}$ population. (E) Expression analysis of pro-inflammatory genes in isolated liver macrophages. Experimental groups are: Obese FD (n = 10), Obese DD (n = 7); NASH FD (n = 10), and NASH DD (n = 9). Data represented as mean ± SD. Groups were compared using the Mann–Whitney test. $^{*}p$ <0.05; $^{**}p$ <0.01. DD, dextran-dexamethasone; FD, Free dextran; FOV, field of view; HepMs, hepatic macrophages; iNOS, inducible nitric oxide synthase; MPO, myeloperoxidase.

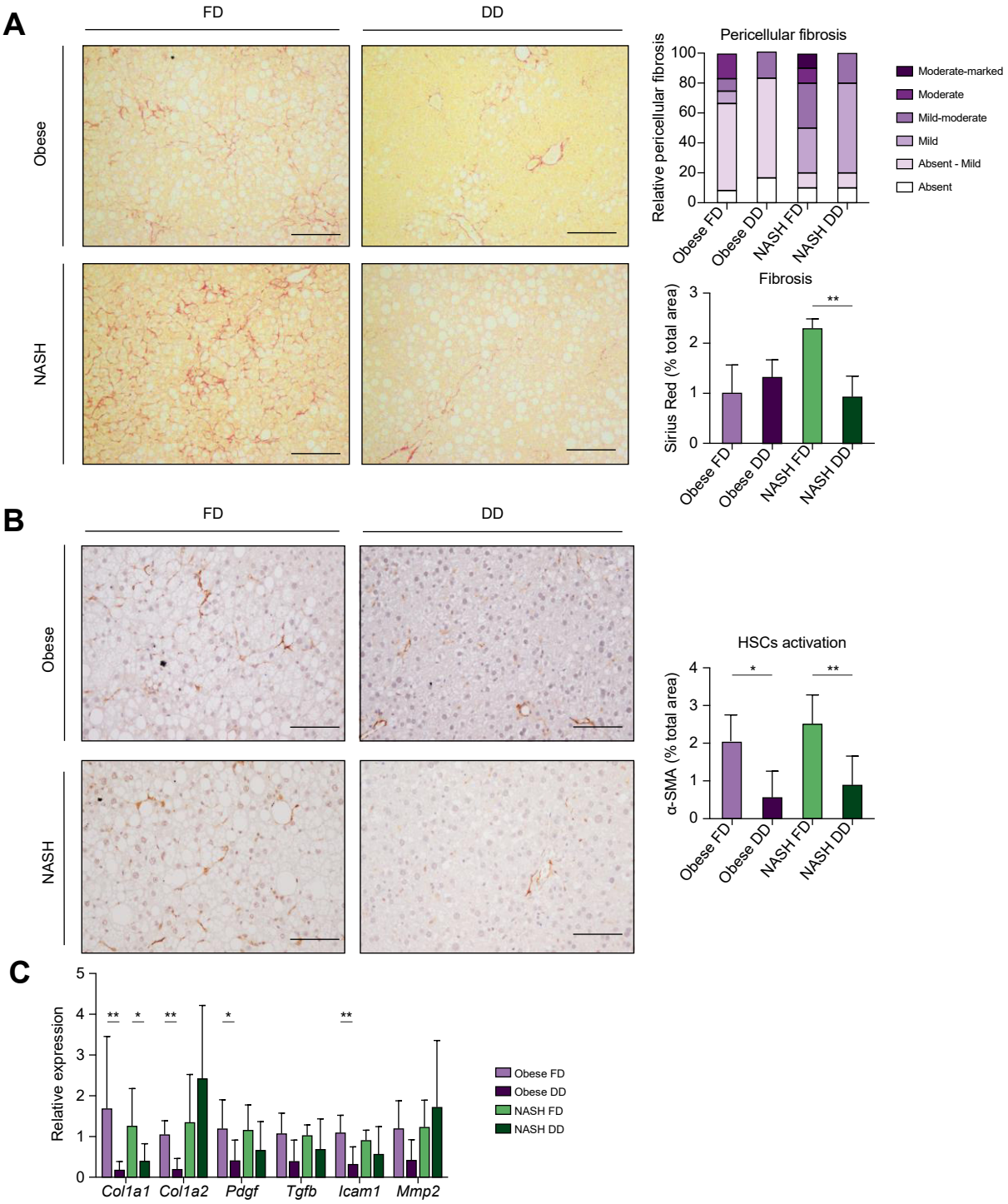

Fig. 5. Chronic dextran-dexamethasone conjugate treatment reduces hepatic fibrosis. (A) Representative images of the Sirius Red staining of liver sections of NASH and obese mice after treatment. Semi-quantitative analysis of pericellular fibrosis and quantification of positively stained area in all experimental groups are shown. (B) Immunohistochemical analysis of αSMA staining and quantification of the stained area in liver sections of obese and NASH mice treated with FD or DD. (C) Relative gene expression analysis of a panel of fibrogenic markers in liver tissue of animals in all experimental groups. Expression values are represented relative to the obese FD group. Animals were grouped in obese FD (n = 10), obese DD (n = 7); NASH FD (n = 10), and NASH DD (n = 9). Data are represented as mean ± SD. Scale bar: 100 μm. The Mann–Whitney test was used to compare experimental groups. $^{*}p$ <0.05 were consider significant; $^{**}p$ <0.01. DD, dextran-dexamethasone; FD, free dextran; NASH, non-alcoholic steatohepatitis.

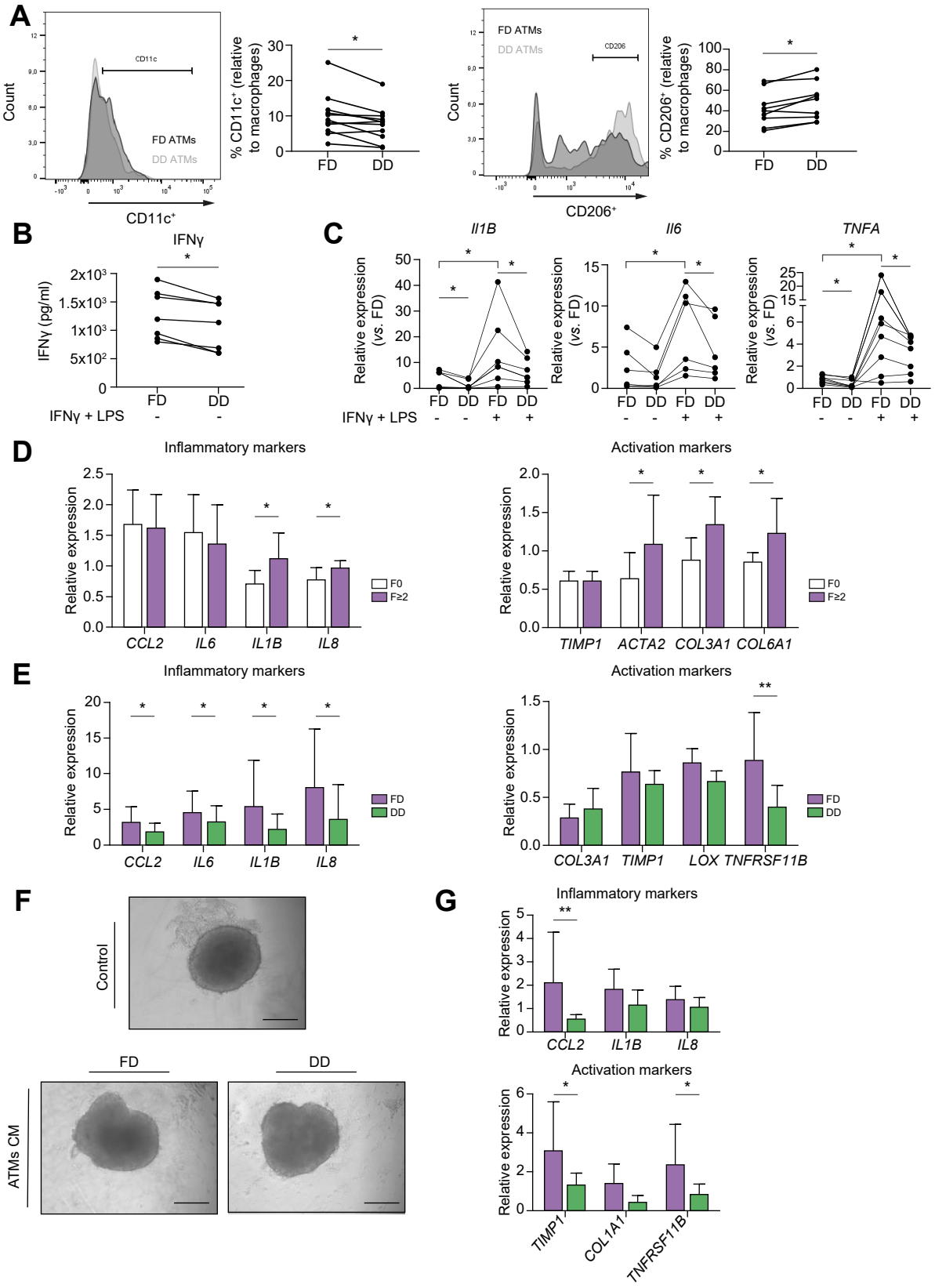

Fig. 6. Human ATMs treated with dextran-dexamethasone conjugates decrease their pro-inflammatory phenotype and reduce hepatic stellate cell activation *in vitro*. (A) Flow cytometry analysis of isolated human ATMs after a 24-h treatment with FD or DD (500 nM). Percentages of CD11c and CD206 cells relative to all macrophages. Obese patients (n = 11) were used for this study. (B) Quantitative analysis of TNFα and IFNγ secretion by ATMs treated with FD or DD (500 nM) measured by ELISA. Replicates per group, n = 7. (C) Relative gene expression analysis of pro-inflammatory markers in human ATMs after FD or DD

whereas the anti-inflammatory phenotype was enriched (p = 0.0117) (Fig. 6A). No differences were observed in FOLR2+ ATMs nor in CD9+ ATMs (Fig. S6). Consistently, the reduction of the pro-inflammatory phenotype was accompanied by a decrease of IFNγ and tumour necrosis factor alpha (TNFα) released by ATMs after DD treatment (Fig. 6B) as measured by ELISA. Furthermore, we confirmed that DD treatment ameliorated the gene expression of the main ATM secreted cytokines (*IL1B, IL6 TNFA*) after they had been polarised to a pro-inflammatory state with LPS and IFNγ (Fig. 6C). Taken together, this indicates that the dexamethasone-nanocarrier treatment *in vitro* effectively reduces the pro-inflammatory phenotype of human ATMs.

Reduction of ATMs pro-inflammatory phenotype influences HSC activation

Human HSCs derived from induced pluripotent cells (iPSC-HSCs) were cultured for 48 h with the ATM secretome collected from patients without hepatic fibrosis (F0) and patients with mild to severe fibrosis (F >2). iPSC-HSCs stimulated with the ATMs secretome from fibrotic patients showed higher expression of the proinflammatory markers *IL1B* (p = 0.036) and *IL8* (p = 0.038) together with higher expression of activation markers *ACTA2, COL3A1,* and *COL6A1* (p = 0.041; p = 0.015 and p = 0.027, respectively) (Fig. 6D). Next, to assess whether the modulation of ATM with DD treatment produced changes on iPSC-HSCs, we collected the supernatant of human ATMs treated with DD or FD for 24 h and added to cultures of iPSC-HSCs. As shown in Fig. 6E the supernatant from DD-treated ATMs reduced iPSC-HSCs gene expression of pro-inflammatory markers (*CCL2*, *IL6*, *IL1B*, *and IL8)* compared with FD-treated ATMs (p = 0.0186; p = 0.0137; p = 0.0234; p = 0.0195, respectively). With respect to fibrosis activation markers, there was a slight decrease in gene expression of *TIMP1* and *LOX2*, and only *TNFRSF11B* showed a significant decrease when the secretome from DD-treated ATMs was used (p = 0.0391, Fig. 6E). Finally, we tested the effects of the ATMs secretome at baseline and after DD modulation using human liver spheroids (iPSC-HSCs and hepatocytes) (Fig. 6F). Gene expression analysis revealed a reduction of inflammatory and fibrogenic responses in iPSC-HSCs as shown by the decreased expression of *CCL2*, *IL8*, *IL1B*, *and COL1A1*, *TIMP1*, *and TNFS11B*, upon DD treatment of ATMs (Fig. 6G). Together, these findings highlight that ATMs might induce hepatic fibrosis by releasing inflammatory cytokines, which contribute to the activation of HSCs and inflammation.

Discussion

Our study reveals a significant association between the degree of liver fibrosis in patients with NAFLD and the abundance of pro-inflammatory macrophages accumulated in the adipose tissue. Moreover, we show that an efficient modulation of the ATM phenotype induced by a recently developed nanomedicine strategy reduces fibrosis progression in a NASH mouse model. Finally, we demonstrate *in vitro* that human ATMs from patients with NAFLD with fibrosis enhance HSC activation and that the modulation of human ATMs with our nanomedicine strategy ameliorates this activation in iPSCs-HSCs and human liver spheroids. Overall, this study reports the direct role of AT inflammation in the progression of the liver fibrosis underlying NAFLD, positioning ATMs as a new therapeutic target to promote fibrosis resolution.

Increasing evidence from animal and human studies have provided confirmation that cytokines released by AT, and more specifically from ATMs, contribute to hepatic and systemic inflammation promoting NAFLD progression to NASH.[10,16,27–32] However, whether ATMs significantly contribute to fibrosis progression in NAFLD is still a major unsolved question. Herein, we included paired liver and adipose tissue biopsies from a unique cohort of patients with NAFLD ranging from F0 to F3–F4. Our results showed a positive correlation between the percentage of ATMs infiltration, mainly with a pro-inflammatory phenotype, and fibrosis in the liver. Given the characteristics of our cohort, the BMI varied significantly between groups with lower BMI in patients with more advanced liver disease and fibrosis. Interestingly, the percentage of inflammatory ATMs in patients with NAFLD was not correlated with BMI but with liver fibrosis, suggesting that it was not the amount of adipose tissue but the inflammation present that affected the liver as has been shown in other chronic metabolic diseases.[12] Recent evidence suggests that subcutaneous AT fibrosis correlates with hepatic fibrosis in NAFLD,[33] however we did not find any correlation between visceral AT fibrosis and liver fibrosis in our cohort. Taken together our results and those of other studies suggest that both subcutaneous and visceral AT may play an important role in human NAFLD, however, the exact contribution and significance of each is not fully understood and should be further explored and compared.

In the present study, we evaluated the effects of targeting ATMs in a NASH model as a strategy to improve liver fibrosis. We used 500 kDa dextran as a nanocarrier to selectively deliver dexamethasone, a potent anti-inflammatory glucocorticoid, to ATMs. The i.p. administration assured that the dextran nanocarriers were predominantly phagocytised by ATMs. Although liver macrophages also captured dextran, the concentration in ATMs was threefold higher compared with their liver counterparts. Interestingly, the retention of the nanocarrier in ATMs was higher in the NASH model and mainly in pro-inflammatory macrophages (CD11c+), most likely because of their enhanced phagocytic capacity and their increased expression of mannose and scavenger receptors known to have a high affinity for high molecular weight dextrans.[23] Chronic treatment with DD conjugates resulted in a reduction of AT inflammatory milieu. Not

(500 nM) treatment under basal or inflammatory conditions (IFNγ + LPS). Replicates per group, n = 7. (D) Gene expression analysis of inflammatory and activation markers in iPSC-HSCs after culture with secretome of ATMs derived from patients without (F0) or with (F>2) fibrosis. Replicates per group n = 10. (E) Gene expression analyses of inflammatory and activation markers in iPSC-HSCs after incubation with conditioned medium (CM) of ATMs treated with FD or DD for 24 h. Replicates per group, n = 10. (F) Representative images of human liver spheroids, containing $HepG_2$ and iPSC-HSCs at a 2:1 ratio, cultured for 48 h with conditioned medium derived from ATMs treated with FD or DD. Scale bar: 100 μm. (G) Gene expression analyses of activation and inflammatory markers in liver spheroids cultured with conditioned medium obtained from human FD- or DD-treated ATMs. Replicates per group, n = 10. ATMs replicates are represented as single values whereas iPSC-HSCs data are represented as mean ± SD. The Wilcoxon test was performed for paired samples comparison (A, B, C) and the Mann–Whitney test was performed for unpaired samples analysis (D, E, G). $^{*}p$ <0.05; $^{**}p$ <0.01. ATMs, adipose tissue macrophages; CM, conditioned medium; DD, dextran–dexamethasone; FD, free dextran; hATMs, human adipose tissue macrophages; IFNγ, interferon gamma; iPSC-HSCs, hepatic stellate cells derived from induced pluripotent stem cells; TNFα, tumour necrosis factor alpha.

only was the overall expression of inflammatory markers decreased but there was also a shift toward ATMs subpopulations. Pro-inflammatory ATMs were reduced, whereas lipid-associated macrophages (LAMs) and tissue resident macrophages were increased. LAMs have been described to reside within crown-like structures and have been associated with the clearing of dying adipocytes[17,34] and therefore we speculate that their increase may have induced adipocyte clearing and reduction of fad pads. Although part of our results can be explained as a consequence of weight loss, the fact that we did not see any differences in the expression of lipid metabolism genes or adipocyte size between groups suggests that targeting ATMs and changing the AT inflammatory milieu played a major role. However, one of the limitations of our study is that we focused on the ATMs phenotype but we did not perform an in-depth characterisation of the changes in AT and systemic metabolism produced by our strategy, which should be explored in future studies.

Notably, the reduction of AT inflammation was associated with an improvement in liver histology, decreasing steatosis, ballooning, and lobular inflammation highlighting the contribution of ATMs to hepatic inflammation. In addition, we observed a reduction of intra-hepatic T cells, while other immune cells such as macrophages and neutrophils remained unaffected. Accordingly, growing evidence indicates that activation of the adaptive immune system plays a key role in triggering the progression of NASH through the secretion of effector cytokines promoting HSC activation and tissue inflammation.[35,36] Although we did not find any differences in the amount of pro-inflammatory hepatic macrophages after DD treatment we did see a discreet reduction of inflammatory markers in isolated hepatic macrophages that could be related to a positive effect of DD on liver macrophages. However, the main effect of DD treatment was on ATMs as demonstrated by the higher degree of ATM dextran engulfment and its phenotype shifting.

More importantly, together with the decrease in liver inflammation, we observed that hepatic fibrosis was radically reduced upon modulation of the ATM phenotype in the NASH model. The reduction of pro-inflammatory ATMs was associated with a decrease in liver collagen content and HSC activation, validating the relationship between $CD11C^{+}$ ATM and liver fibrosis degree observed in our cohort of patients with NAFLD. Although the improvement of liver histology can be explained in part as a consequence of weight loss, our results suggest that the modulation of ATMs played a major role. In fact, NASH-DD animals and Obese-DD animals lost similar amounts of weight but NASH animals exhibited higher dextran engulfment and a significant reduction of *Il6*, *Il1b*, and *Tnfa* gene expression in isolated ATMs that was associated with a significant decrease in liver fibrosis, while obese animals did not. Collectively, these results demonstrate the potential of ATMs as inducers of hepatic fibrosis and position ATMs as potential therapeutic targets to reduce fibrosis in NAFLD.

To evaluate whether our findings may be transferable to human ATMs we confirmed that the ATMs secretome from patients with NAFLD with fibrosis induced higher activation of HSCs compared with patients without fibrosis. Moreover, *in vitro* treatment of human ATMs with DD promoted their shift to a more anti-inflammatory phenotype and reduced cytokine release (IFNγ and TNFα). Interestingly, we found that the expression of the TNF receptor superfamily 11B (*TNFRSF11B*) gene was upregulated in liver spheroids when incubated with conditioned medium from ATMs and returned to baseline values when cultured with the secretome of DD-treated ATMs. Of note, TNFRSF11B expression is mediated by TNFα signalling through the TNFR1 and is found to be upregulated in human-activated HSCs compared with their quiescent counterparts.[37]

In conclusion, in this study we uncovered a direct link between pro-inflammatory macrophages of AT and fibrosis progression in NAFLD. In addition, we demonstrated that chronic modulation of the pro-inflammatory phenotype of ATMs elicited a profound effect on liver fibrosis regression in a NASH experimental model. Finally, we demonstrated the ability of the ATMs secretome to induce the activation of human HSCs. Collectively our data provide evidence that targeting ATMs might represent a novel approach to tackling liver fibrosis progression in NAFLD.

Abbreviations

α-SMA, α-smooth muscle actin; ALP, Alkaline phosphatase; ALT, Alanine aminotransferase; AST, Aspartate aminotransferase; ATM, Adipose tissue macrophages; DD, Dextran-dexamethasone; FD, Free drug dextran; FOV, Field of view; HepMs, Hepatic macrophages; HSCs, Hepatic stellate cells; HFD, High-fat diet; HFHCD, High-fat high-cholesterol diet; HTN, Hypertension; IFNγ, Interferon-gamma; iPSC-HSCs, Hepatic stellate cells derived from induced pluripotent stem cells; LPS, Lipopolysaccharide; MCP1, Monocyte chemoattractant protein 1; MPO, Myeloperoxidase; NAFLD, Non-alcoholic fatty liver disease; NASH, Non-alcoholic steatohepatitis; TNFα, Tumour necrosis factor-alpha; TNFRSF11B, Tumour necrosis factor receptor superfamily; VAT, Visceral adipose tissue.

Financial support

This work was supported by grants from Fondo de Investigación Sanitaria Carlos III (FIS) and co-financed by the Fondo Europeo de Desarrollo Regional (FEDER), Unión Europea, 'Una manera de hacer Europa' (PI18/00862 to I.G and M.C, and PI22/00776 to IG). PS-B was funded by Instituto de Salud Carlos III; PI20/00765. BA was funded by Instituto de Salud Carlos III, PFIS (FI16/00203); and MC was funded by Ramon y Cajal programme from the Ministerio de Ciencia e Innovación RYC2019-026662-I and by Plan estatal de investigación científica y técnica de innovación PID2021-125195OB-I00. AS acknowledges support from the U.S. National Institutes of Health (NIH R01 DK112251 and R01 EB032249).

Conflicts of interest

All authors declare no conflicts of interest related to this manuscript.

Please refer to the accompanying ICMJE disclosure forms for further details.

Authors' contributions

Participated in the design of this study: CM-S, AS. Followed the study: PG. Participated in patient recruitment and patient stratification: OB. Collected clinical data: NJ, AJ, MC, MP, AS, and EP. Contributed to the obtention of patients' samples: JF, JV, YF, FJSM. . Synthesised and characterised the dextran conjugates: HD. Performed and supervised experiments: AS. Performed experiments: CM-S. Helped with the experiments performed: XA, DB, RM, SA, BA-B, JV, AG, LA, OS-C. Performed the blinded histological analysis of mice samples: CM. Contributed to the animal model: VH. Drafted the manuscript: CM-S. Critically reviewed the manuscript: KS, SA, PS-B, PG, AS. Conceived and designed the study: IG, MC. Supervised the study: IG, MC.

Data availability statement

The data generated from the studies are available from the corresponding author on reasonable request.

Acknowledgements

This work was performed in the Centre Esther Koplowitz (CEK) and the dextran conjugates were synthesised in the University of Illinois. The authors wish to thank Flor Apolino for her support in collecting samples at the Hospital Clinic of Barcelona. We are indebted to the Cytomics Unit, Genomics Unit and Biobank core facility of the Fundació Clinic per la Recerca Biomèdica-Institut d'Investigacións Biomèdiques August Pi i Sunyer (FCRB-IDIBAPS) for technical help.

Supplementary data

Supplementary data to this article can be found online at https://doi.org/10.1016/j.jhepr.2023.100830.

References

Author names in bold designate shared co-first authorship

[1] Tacke F, Weiskirchen R. Non-alcoholic fatty liver disease (NAFLD)/non-alcoholic steatohepatitis (NASH)-related liver fibrosis: mechanisms, treatment and prevention. Ann Transl Med 2021;9:729.
[2] Younossi ZM, Koenig AB, Abdelatif D, Fazel Y, Henry L, Wymer M. Global epidemiology of nonalcoholic fatty liver disease—meta-analytic assessment of prevalence, incidence, and outcomes. Hepatology 2016;64:73–84.
[3] Angulo P, Machado MV, Diehl AM. Fibrosis in nonalcoholic fatty liver disease: mechanisms and clinical implications. Semin Liver Dis 2015;35:132–145.
[4] Heyens LJM, Busschots D, Koek GH, Robaeys G, Francque S. Liver fibrosis in non-alcoholic fatty liver disease: from liver biopsy to non-invasive biomarkers in diagnosis and treatment. Front Med 2021;8:615978.
[5] Dulai PS, Singh S, Patel J, Soni M, Prokop LJ, Younossi Z, et al. Increased risk of mortality by fibrosis stage in nonalcoholic fatty liver disease: systematic review and meta-analysis. Hepatology 2017;65:1557–1565.
[6] Nobili V, Svegliati-Baroni G, Alisi A, Miele L, Valenti L, Vajro P. A 360-degree overview of paediatric NAFLD: recent insights. J Hepatol 2013;58:1218–1229.
[7] Nakajima S, Koh V, Kua L-F, So J, Davide L, Lim KS, et al. Accumulation of CD11c+CD163+ adipose tissue macrophages through upregulation of intracellular 11β-HSD1 in human obesity. J Immunol 2016;9:3735–3745.
[8] Wouters K, Gaens K, Bijnen M, Verboven K, Jocken J, Wetzels S, et al. Circulating classical monocytes are associated with CD11c+ macrophages in human visceral adipose tissue. Sci Rep 2017;7:1–8.
[9] Boutens L, Hooiveld GJ, Dhingra S, Cramer RA, Netea MG, Stienstra R. Unique metabolic activation of adipose tissue macrophages in obesity promotes inflammatory responses. Diabetologia 2018;61:942–953.
[10] Du Plessis J, Van Pelt J, Korf H, Mathieu C, Van Der Schueren B, Lannoo M, et al. Association of adipose tissue inflammation with histologic severity of nonalcoholic fatty liver disease. Gastroenterology 2015;149:635–648.e14.
[11] Rosso C, Kazankov K, Younes R, Esmaili S, Marietti M, Sacco M, et al. Crosstalk between adipose tissue insulin resistance and liver macrophages in non-alcoholic fatty liver disease. J Hepatol 2019;71:1012–1021.
[12] Chait A, den Hartigh LJ. Adipose tissue distribution, inflammation and its metabolic consequences, including diabetes and cardiovascular disease. Front Cardiovasc Med 2020;7:22.
[13] Bijnen M, Josefs T, Cuijpers I, Maalsen CJ, Van De Gaar J, Vroomen M, et al. Adipose tissue macrophages induce hepatic neutrophil recruitment and macrophage accumulation in mice. Gut 2018;67:1317–1327.
[14] Negi CK, Babica P, Bajard L, Bienertova-Vasku J, Tarantino G. Insights into the molecular targets and emerging pharmacotherapeutic interventions for nonalcoholic fatty liver disease. Metabolism 2022;126:154925.
[15] Fontana L, Eagon JC, Trujillo ME, Scherer PE, Klein S. Visceral fat adipokine secretion is associated with systemic inflammation in obese humans. Diabetes 2007;56:1010–1013.
[16] Lefere S, Tacke F. Macrophages in obesity and non-alcoholic fatty liver disease: crosstalk with metabolism. JHEP Rep 2019;1:30–43.
[17] **Jaitin DA**, **Adlung L**, **Thaiss CA**, **Weiner A**, **Li B**, et al. Lipid-associated macrophages control metabolic homeostasis in a Trem2-dependent manner. Cell 2019;178:686–698.e14.
[18] Ying W, Riopel M, Bandyopadhyay G, Dong Y, Birmingham A, Seo JB, et al. Adipose tissue macrophage-derived exosomal miRNAs can modulate in vivo and in vitro insulin sensitivity. Cell 2017;171:372–384.e12.
[19] Wang YYY, Tang B, Long L, Luo P, Xiang W, Li X, et al. Improvement of obesity-associated disorders by a small-molecule drug targeting mitochondria of adipose tissue macrophages. Nat Commun 2021;12:1–16.
[20] Marchesini G, Day CP, Dufour JF, Canbay A, Nobili V, Ratziu V, et al. EASL–EASD–EASO Clinical Practice Guidelines for the management of non-alcoholic fatty liver disease. J Hepatol 2016;64:1388–1402.
[21] Chalasani N, Younossi Z, Lavine JE, Charlton M, Cusi K, Rinella M, et al. The diagnosis and management of nonalcoholic fatty liver disease: practice guidance from the American Association for the Study of Liver Diseases. Hepatology 2018;67:328–357.
[22] Ampem G, Röszer T. Isolation and characterization of adipose tissue macrophages. Methods Mol Biol 2019;1966:225–236.
[23] Ma L, Liu TW, Wallig MA, Dobrucki IT, Dobrucki LW, Nelson ER, et al. Efficient targeting of adipose tissue macrophages in obesity with polysaccharide nanocarriers. ACS Nano 2016;10:6952–6962.
[24] **Vallverdú J**, **Martínez García de la Torre RA**, et al. Directed differentiation of human induced pluripotent stem cells to hepatic stellate cells. Nat Protoc 2021;16:2542–2563.
[25] Pustylnikov S, Sagar D, Jain P, Khan ZK. Targeting the C-type lectins-mediated host-pathogen interactions with dextran. J Pharm Pharm Sci 2014;17:371–392.
[26] Kleiner DE, Brunt EM, Van Natta M, Behling C, Contos MJ, Cummings OW, et al. Design and validation of a histological scoring system for nonalcoholic fatty liver disease. Hepatology 2005;41:1313–1321.
[27] Deng H, Konopka CJ, Prabhu S, Sarkar S, Medina NG, Fayyaz M, et al. Dextran-mimetic quantum dots for multimodal macrophage imaging in vivo, ex vivo, and in situ. ACS Nano 2021;16:1999–2012.
[28] Polyzos SA, Kountouras J, Mantzoros CS. Adipokines in nonalcoholic fatty liver disease. Metabolism 2016;65:1062–1079.
[29] Adolph TE, Grander C, Grabherr F, Tilg H. Adipokines and non-alcoholic fatty liver disease: multiple interactions. Int J Mol Sci 2017;18:1237.
[30] Tordjman J, Divoux A, Prifti E, Poitou C, Pelloux V, Hugol D, et al. Structural and inflammatory heterogeneity in subcutaneous adipose tissue: relation with liver histopathology in morbid obesity. J Hepatol 2012;56:1152–1158.
[31] Cancello R, Tordjman J, Poitou C, Guilhem G, Bouillot JL, Hugol D, et al. Increased infiltration of macrophages in omental adipose tissue is associated with marked hepatic lesions in morbid human obesity. Diabetes 2006;55:1554–1561.
[32] Wentworth JM, Naselli G, Brown WA, Doyle L, Phipson B, Smyth GK, et al. Pro-inflammatory CD11c+CD206+ adipose tissue macrophages are associated with insulin resistance in human obesity. Diabetes 2010;59:1648–1656.
[33] Beals JW, Smith GI, Shankaran M, Fuchs A, Schweitzer GG, Yoshino J, et al. Increased adipose tissue fibrogenesis, not impaired expandability, is associated with nonalcoholic fatty liver disease. Hepatology 2021;74:1287–1299.
[34] **Hill DA**, **Lim HW**, et al. Distinct macrophage populations direct inflammatory versus physiological changes in adipose tissue. Proc Natl Acad Sci U S A 2018;115:E5096–E5105.
[35] Hirsova P, Bamidele AO, Wang H, Povero D, Revelo XS. Emerging roles of T cells in the pathogenesis of nonalcoholic steatohepatitis and hepatocellular carcinoma. Front Endocrinol 2021;12:760860.
[36] Ramadori P, Kam S, Heikenwalder M. T cells: friends and foes in NASH pathogenesis and hepatocarcinogenesis. Hepatology 2022;75(4):1038–1049.
[37] Wang ZY, Keogh A, Waldt A, Cuttat R, Neri M, Zhu S, et al. Single-cell and bulk transcriptomics of the liver reveals potential targets of NASH with fibrosis. Sci Rep 2021;11:19396.
[38] Titos E, Rius B, González-Périz A, López-Vicario C, Morán-Salvador E, Martínez-Clemente M, et al. Resolvin D1 and its precursor docosahexaenoic acid promote resolution of adipose tissue inflammation by eliciting macrophage polarization toward an M2-like phenotype. J Immunol 2011;187:5408–5418.